Theoretical Modeling and Simulation of a Chaos-Based Physical Layer for WSNs

Stevan Berber, Shu Feng

***Abstract*—** In this paper the theoretical model and simulation of the physical layer for wireless sensor networks (WSNs) application is presented. The spreading sequences used are generated from the chaotic generators design using Chebyshev maps that increases the security in signal transmission. Signal propagation in WSNs assumes heavy influence of fading and inter-symbol interference. To mitigate this fading influence the application of chip interleaving technique is applied. For the case of fading presence in the channel and the case of interleaver application, the theoretical expressions for the bit error rate (BER) in closed form are derived. The system simulators are developed that confirmed theoretical findings. The signal processing procedures in the transmitter and receiver blocks are presented in discrete time domain that makes the design of devices directly implementable in DSP technology, which was one of the aims of this research.

***Keywords*—**Chaos based systems, fading channel, probability of error, wireless sensor networks, interleavers.

I. INTRODUCTION

THIS paper presents the issues in physical layer design for application in wireless sensor networks (WSNs). One of the basic requirements in these networks is to design network nodes with minimum power consumption. The main cause for increased power consumption in signal transmission is related to the existence of fading in communication channel. This increase for transmission power can be tens of decibels. It was proved that the fading can be quantified through the increase of BER in the physical layer in respect to the case when only additive Gaussian noise (AWGN) is present in the channel.

For the desired BER in the wireless networks, the power of nodes needs to increase in the presence of fading in order to communicate at the same distance [1]. The aim of the network designer is to reduce this increase in required power. Various techniques of fading mitigation are used to achieve this aim. It was shown that the fading influence in direct sequence spread spectrum and CDMA systems can be reduced by using interleaving techniques [2, 3, 4, 5, 6]. A wireless sensor network defined in the Standard IEE 802.15.4 [7] uses a modified spread spectrum technique. For that reason an analysis of implementing chaotic sequences generated using logistic and cubic maps is presented. To mitigate fading in the communication channel a chip interleaving technique is investigated.

One solution for the design of modulator and demodulator blocks for wireless sensor networks application is presented in [8]. The paper presented theoretical modeling, simulation and design of the blocks in FPGA technology and implementation in CMOS technology. The transceiver design for WSNs applications is presented in [9].

In contrast to these designs, this paper is unique in presenting the theoretical analysis and simulation of the physical layer of WSNs in discrete time domain, which is the first contribution of this paper. This presentation is suitable for use in direct implementation of the systems blocks in DSP or FPGA technology. In the existing theory these signals and their processing are represented in continuous time form. The second contribution of this paper is in theoretical analysis of the whole system and derivations of BER expressions for chaotic spreading sequence for both AWG noise and fading channels. The third contribution is in the development of the system's simulator which confirmed theoretically expected signal waveforms and BER expressions.

The theoretical model of the chaos-based system in presence of noise and fading is presented in Section 2. In particular the basic chaotic maps are explained and the basic properties of the chaotic sequences are presented. Section 3 presents the basic structure of the system and its mathematical model in the case when noise and fading are present in the channel. The theoretical BER curves are confirmed by simulation. In Section 4 the interleaver and deinterleaver blocks are included into the transmitter and receiver structures respectively. For this case the expressions for the BER are derived in closed forms Also, the results of BER simulation are presented, which confirmed the theoretical findings. Conclusions are presented in Section 5.

II. THEORETICAL MODEL OF CHAOS-BASED PHYSICAL LAYER

A. Definition of Chaotic Sequences

Chaotic sequences are non-binary sequences. The statistical structure of these sequences depends on the defined initial conditions. These sequences can be used as spreading sequences in direct sequences spread-spreading systems DSSS) and in code-division multiple access systems (CDMA) [1, 2, 4, 5]. Due to their correlation properties, these chaotic sequences, generated using chaotic maps, can be used in these systems to spread message bits, if the synchronization of the

Stevan Berber is with the Department of Electrical and Computer Engineering, The University of Auckland, Auckland, New Zealand, (corresponding author, phone: +64 923 8966; fax: +64 373 7461; e-mail: s.berber@auckland.ac.nz).

Shu Feng is with the Department of Communication Engineering, EEOT, Nanjing University of SCI and TECH, Nanjing, China (e-mail: shufeng@mail.njust.edu.cn).

sequences is achieved [10, 12]. The chaotic mapping called Chebyshev Degree-L maps is defined by this recursive equation

$$c(k+1) = \cos[L\cos^{-1}c(k)]\,. \tag{1}$$

The discrete random samples in the sequence $c(k)$ have the values between -1 and +1. For L = 2 the logistic map is obtained, and the samples for this map are generated according to this recursive expression

$$x_{k+1} = 2x_k^2 - 1 \tag{2}$$

For L = 3 the cubic map is defined. The samples for this map are generated according to this recursive expression

$$x_{k+1} = 3x_k(1 - x_k^2) \tag{3}$$

The density function for these maps is

$$f_C(c) = \frac{1}{2\sqrt{1-c^2}} \tag{4}$$

The analytical results and simulations, which are presented in this paper, are based on the logistic map. The discrete random values in a chaotic sequence will represent chips in the spreading sequences. The series of chips can be treated as a discrete time stochastic process. The mean value of this process is zero and the mean square value, corresponding to the power of the sequence, is 0.5.

In order to compare chaotic systems with the classical binary system the chaotic generator needs to produce the chaotic chips carrying the same average power as the power of the binary sequence. For that reason, in this paper, the chaotic samples are generated with the average power one. Thus the random variable, defining the samples of the chaotic sequence, in this paper denoted by c_{i1}, is defined as a linear function of c, i.e., $c_{i1}(k) = \sqrt{2}c(k)$. Using the fundamental theorem of probability theory the density function of c_{i1} is derived as

$$f_{C_{i1}}(c_{i1}) = \frac{1}{\pi\sqrt{2-c_{i1}^2}}\,, \text{ for } -\sqrt{2} \le c_{i1} \le \sqrt{2}\,, \tag{5}$$

which is presented in Fig. 1. It is symmetric in respect to zero and can have the values between plus minus square root of two. The mean value of this random variable is

$$E\{c_{i1}\} = \int_{-\sqrt{2}}^{\sqrt{2}} c_{i1} \frac{1}{\pi\sqrt{2-c_{i1}^2}} dc_{i1} = 0\,. \tag{6}$$

and the average power is

$$E\{c_{i1}^2\} = \int_{-\sqrt{2}}^{\sqrt{2}} c_{i1}^2 \frac{1}{\pi\sqrt{2-c_{i1}^2}} dc_{i1} = 1 \tag{7}$$

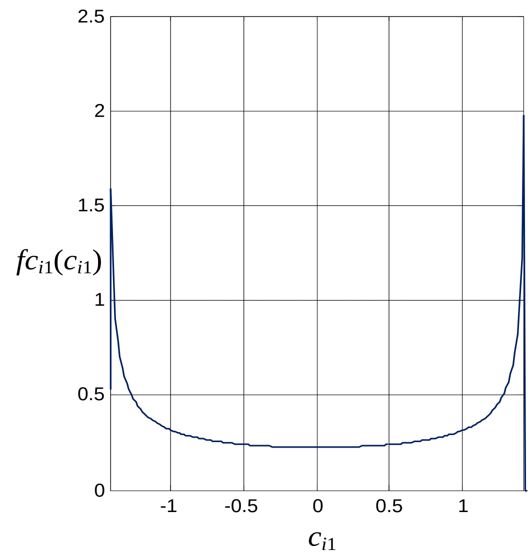

Fig. 1. Density function of chaotic random variable

For the derivatives of BER expression this expectation will be used

$$E\{c_{i1}^4\} = \int_{-\sqrt{2}}^{\sqrt{2}} c_{i1}^4 \frac{1}{\pi\sqrt{2-c_{i1}^2}} dc_{i1} = \frac{3}{2}\,. \tag{8}$$

B. Block-schematic of the communication system

The proposed modulation schemes in wireless sensor networks are the binary and quadrature phase shit keying (BPSK and QPSK). Fig. 2 presents a simplified block schematic of a system that uses offset QPSK (OQPSK) modulation and chaotic spreading sequences instead of the standard binary sequences proposed for wireless sensor networks [7]. The system will be, firstly, analyzed for the case when the Additive White Gaussian Noise (AWGN) and fading are present in the channel. Secondly, the system will be analyzed for the case when interleaver (IL) and deinterleaver (DI) blocks are incorporated into the block schematic in Fig. 2.

C. Transmitter operation

The transmitter operates in the following way. The source generates message bits $b_{j1}(k)$, which are spread by the chaotic spreading sequence $c_{in}(k)$ and a chip sequence $m(k)$ = $b_{j1}(k)c_{i1}(k)$ is obtained. A demultiplexer block (DMUX) is used to split the chip sequence $m(k)$ into in-phase and quadrature sequences as specified by the Standard for wireless sensor networks [7]. The even-indexed chip sequence $m_I(k)$ modulates the in-phase carrier and odd-indexed chip sequence $m_Q(k)$ modulates the quadrature carrier. The output of the modulator is the QPSK signal expressed as

$$s(k) = m_I(k)\sqrt{2E_c / M} \cdot \cos\Omega_c k + m_Q(k)\sqrt{2E_c / M} \cdot \sin\Omega_c k \quad (9)$$

where $m_I(k)$ and $m_Q(k)$ are in-phase and quadrature chip sequences respectively, and Ω_c is the normalized frequency of the carrier.

The energy of a bit is $E_b = 2\beta E_c$, where E_c is the energy per chip. The number of interpolated samples contained in one chip interval is M. It is important to see that the system is analyzed for discrete time domain signal representation, i.e., each chip and related noise sample are generated once for each chip interval and then repeated (interpolated) M times in the chip interval to allow the discrete time modulation of the carrier.

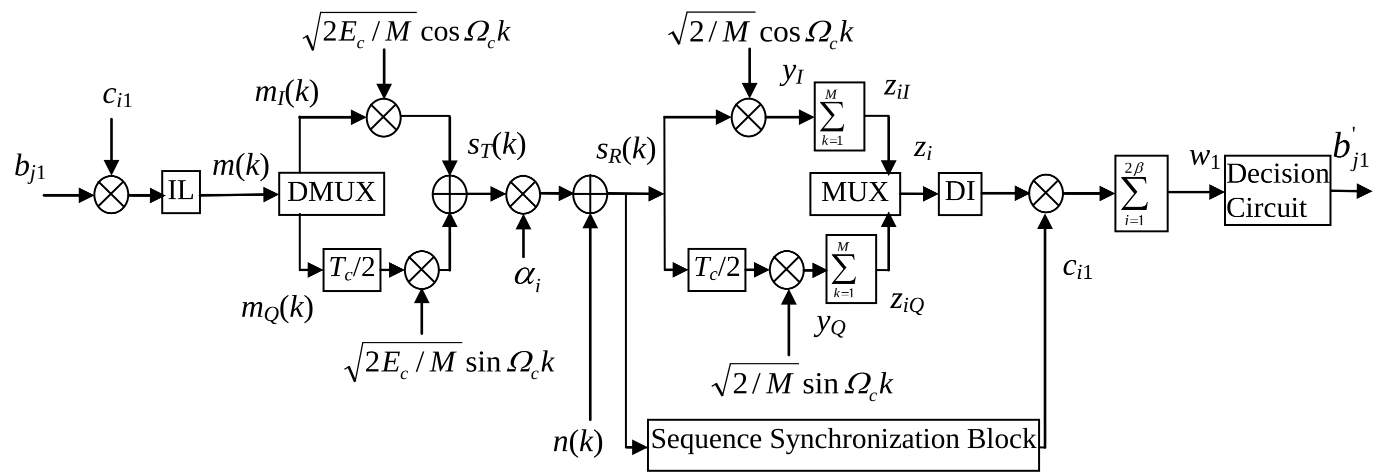

Fig. 2 Block schematic of communication system

D. Channel characterization

A noise sample is generated in each chip interval and then is repeated M times and added to M identical chaotic samples representing a chip. For M repeated samples of noise in a chip interval the average energy is $E_N = M\sigma^2$, where the variance is $\sigma^2 = BN_0$ and the bandwidth B=1/2T_c=1/2M. Thus, the energy of a noise in a chip interval is calculated to be $E_N = N_0/2$. The band-limited pass-band noise samples are generated in discrete time domain according to this expression

$$n(k) = n_I(k)\sqrt{2E_N / M} \cdot \cos\Omega_c k - n_Q(k)\sqrt{2E_N / M} \cdot \sin\Omega_c k, \quad (10)$$

which corresponds to the block schematic presented in Fig. 3.

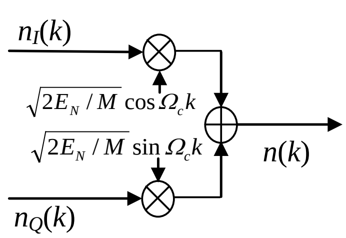

Fig. 3 Pass-band noise generator

The noise components $n_I(k)$ and $n_Q(k)$ are in-phase and quadrature noise samples of zero mean and unit variance. The energy of the noise samples inside a chip interval is E_N and M is the number of interpolated samples inside the chip interval. Thus, the output of the noise generator in Fig. 3 is the pas-band noise with the frequency bandwidth that corresponds to the bandwidth of the generated signal. Also, in the system simulation the power of the noise is contolled by defining the value of the noise energy E_N.

If fading is present in the channel it is represented by a multiplier in Fig. 2. The incoming transmitted signal is multiplies by a fading coefficient α which is a realization of a random variable that has Rayleigh density function defined as

$$f_\alpha(\alpha) = \frac{2\alpha}{b} e^{-\alpha^2/b}. \quad (11)$$

Defined by this density function, the random variable α has the mean value $\eta_\alpha = (\pi b/4)^{-1/2}$ and variance $\sigma^2_\alpha = b(4-\pi)/4$.

E. Correlator receiver operation

If fading is present in the channel, the received signal $s_R(k)$ is [3]

$$s_R(k) = \alpha e^{-j\varphi} s(k) + n(k) \quad (12)$$

where α is the fading coefficient and φ is the phase shift. For a slow fading it is assumed that the fading coefficient is constant in a bit interval, It is also assumed that the phase shift φ can be eliminated by the receiver's phase locked loop. The received signal $s_R(k)$ can be coherently demodulated using a correlator receiver which consists of a multiplier and an adder. The signal at the output of the multiplier in in-phase branch is

$$y_I(k) = [\alpha s(k) + n(k)]\sqrt{2E_c / M} \cdot \cos \Omega_c k \tag{13}$$

The M samples inside a chip interval of this discrete signal are added (corresponds to integration in continuous time systems) resulting in a random sample z_i in I branch for even index values i = 2, 4,…, β. The similar processing is performed in the Q branch for i = 1, 3,…,β-1. The multiplexer (MUX) combines in-phase and quadrature sequences back into a 2β-chip sequence of samples that is represented by this realization of a discrete time stochastic process Z_i

$$z_i = \alpha\sqrt{E_c} \cdot c_{i1} + \sqrt{E_N} \cdot n_i \tag{14}$$

where i = 1, 2, 3, 4,…, 2β and n_i are samples of the in-phase and quadrature baseband noise. The first term in this sample represents the signal part and the second one is the noise part.

In order to detect the bit values the incoming stream of chips, representing a bit, needs to be correlated with the locally generated and synchronized reference chip sequence. Therefore, the received stream of discrete samples z_i is correlated with a locally generated reference chip sequences (c_{i1}, i = 1, 2, 3, 4, … , 2β), obtained from the sequences synchronization block [10, 12]. The correlator consists of a multiplier and an adder. For the sake of simplicity, it is assumed that the bit sent was +1. Then the output of adder will be a random sample that represents a soft bit received value and is expressed as

$$\begin{aligned} w_1 &= \sum_{i=1}^{2\beta} z_i c_{i1} = \alpha\sqrt{E_c}\sum_{i=1}^{2\beta} c_{i1}^2 + \sqrt{E_N}\sum_{i=1}^{2\beta} n_i \cdot c_{i1} \\ &= A + B \end{aligned} \tag{15}$$

III. Communication systems with Noise and fading

A. Closed form BER derivation for cubic map

It is assumed that the source generates binary bits from the alphabet (+1, -1). The received soft bit values will be represented as a discrete time stochastic process with the samples representing realizations of a random variable W_1. The mean value of this random variable is zero. Thus, the threshold value in the decision circuit should be defined as $z_{iT} = 0$.

Assuming that the bit sent is +1, the density function of random variable W_1, due to the central limit theorem (CLT), can be approximated by Gaussian function. Also, assuming that the powers of all chips are equal, the mean value of W_1 may be calculated as

$$\eta_{w_1} = E\{w_1\} = \sqrt{E_c}E\{\alpha\}\sum_{i=1}^{2\beta} E\{c_{i1}^2\} \tag{16}$$

and the variance of in general form as

$$\sigma_{w1}^2 = E\{w_1^2\} - \eta_{w1}^2 = E\{(A+B)^2\} - \eta_{w1}^2 . \tag{17}$$

It can be found

$$\begin{aligned} E\{A^2\} &= \left\{\left[\alpha\sqrt{E_c}\sum_{i=1}^{2\beta} c_{i1}^2\right]^2\right\} \\ &= 2\beta E\{\alpha^2\}E_c[E\{c_{i1}^4\} + (2\beta-1)E\{c_{i1}^2\}E\{c_{j1}^2\}] \end{aligned} \tag{18}$$

and

$$E\{B^2\} = E\left\{\left[\sqrt{E_N}\sum_{i=1}^{2\beta} n_i \cdot c_{i1}\right]^2\right\} = 2\beta E_N E\{c_{i1}^2\} \tag{19}$$

The mean value squared can be expressed in this form

$$\begin{aligned} \eta_{w1}^2 &= E^2\{w_1\} = 2\beta E_c E^2\{\alpha\}E^2\{c_{i1}^2\} \\ &\quad + 2\beta(2\beta-1)E_c E^2\{\alpha\}E^2\{c_{i1}^2\}E^2\{c_{j1}^2\} + \sum_{i=1}^{2\beta} E\{c_{i1}^2\} \end{aligned} \tag{20}$$

The variance can be obtained from (17), (18), (19) and (20) in this form

$$\begin{aligned} \sigma_{w1}^2 &= 2\beta E_c[E\{\alpha^2\}E\{c_{i1}^4\} - E^2\{\alpha\}E\{c_{i1}^2\}] \\ &\quad + 2E_c[E\{\alpha^2\} - E^2\{\alpha\}]\sum_{i=1}^{2\beta} E\{c_{i1}^2\}\sum_{j=i+1}^{2\beta} E\{c_{j1}^2\} \\ &\quad + 2\beta E_N E\{c_{i1}^2\} \end{aligned} \tag{21}$$

Suppose that the cubic map is used. Inserting the values from expressions (7) and (8), and the values for the expectations of the fading coefficient α, the expression for the variance can be simplified as

$$\sigma_{w1}^2 = 2\beta E_c[\frac{\pi-2}{4} + \beta(4-\pi) + \frac{N_0}{2E_c}] . \tag{22}$$

Having the mean and variance available, the probability bit error can be expressed as

$$p_{be} = \frac{1}{2}erfc\left[\frac{\pi-2}{\beta\pi} + \frac{4(4-\pi)}{\pi} + \frac{4}{\pi}\left(\frac{E_b}{N_0}\right)^{-1}\right]^{-1/2} \tag{23}$$

where the energy of a bit is $E_b = 2\beta E_c$ and energy of the noise is $E_N = N_0/2$.

B. System simulation and comparison with theory

The simulators of the systems, including pulse shaping, are developed and simulations were conducted for various channel conditions. The system is simulated in MATLAB and the resultant BER curves are generated and plotted alongside with the theoretical curves.

For the case when anly WGN is present in the channel, the graphs, showing theoretical probability of error and the simulated BER values, are presented in Fig. 4. The graph obtained by simulation follows the shape of the graph for theoretical BPSK modulation as expected. Namely, when fading influence is eliminated, $\alpha = 1$, and the noise only is present in the channel, the theoretical expression (5) becomes,

$$z_i = \sqrt{E_c} \cdot c_{i1} + \sqrt{E_N} \cdot n_i \tag{24}$$

Because the influence of fading is eliminated, the output of adder, representing a soft bit received value, can be expressed from (15) as

$$\begin{aligned} w_1 &= \sum_{i=1}^{2\beta} z_i c_{i1} = \sqrt{E_c} \sum_{i=1}^{2\beta} c_{i1}^2 + \sqrt{E_N} \sum_{i=1}^{2\beta} n_i \cdot c_{i1} \\ &= A + B \end{aligned} \tag{25}$$

The density function of random variable W_1 is Gaussian. If the powers of all chips are equal, the mean value of W_1 may be calculated from (16) as

$$\eta_{w_1} = E\{w_1\} = 2\beta E\{c_{i1}^2\}\sqrt{E_c} = 2\beta\sqrt{E_c}\,. \tag{26}$$

and the variance (17), for expected values specified in (26), can be calculated as

$$\begin{aligned} \sigma_{w1}^2 &= 2\beta E_c[E\{c_{i1}^4\} - E\{c_{i1}^2\}] + 2\beta E_N E\{c_{i1}^2\} \\ &= 2\beta E_c[3/2 - 1] + 2\beta E_N = \beta E_c + 2\beta E_N \end{aligned} \tag{27}$$

For the mean and variance calculated, the probability bit error can be expressed as

$$p_{be} = \frac{1}{2} erfc\left[\frac{1}{2\beta} + \left(\frac{E_b}{N_0}\right)^{-1}\right]^{-1/2} \tag{28}$$

where the energy of a bit is $E_b = 2\beta E_c$ and energy of the noise is $E_N = N_0/2$.

The graphs in Fig. 4 and Fig. 5 are closely approximate the theoretical BER curve. However this approximation is different for the two plots presented. The reason is in that, during the simulation, the initial condition for chaotic sequence generation was different, because the simulator randomly generates initial condition.

To clarify this fact, Fig. 5 presents four simulations of the BER curves. Obviously they are close to the theoretical curve, still being at different position in respect to that curve.

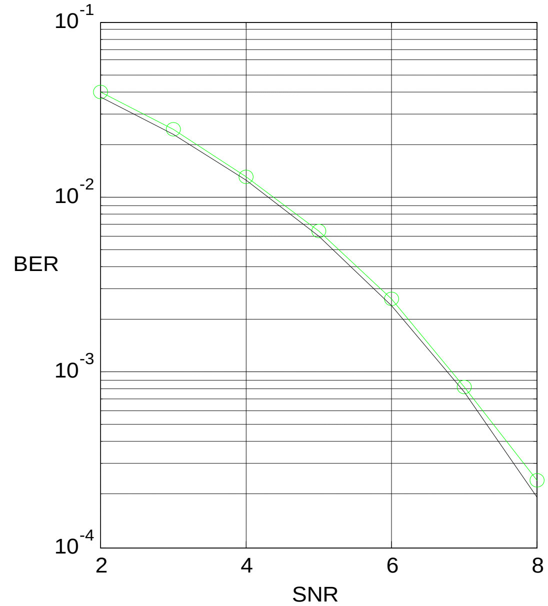

Fig. 4 BER curves for the chaotic receiver in presence of AWGN: theoretical (black) and simulation (green).

The theoretical BER (blue) in presence of fading for binary chip spreading and transmission is compared with the BER obtained by derived formula (12) (magenta) for chaotic chips spreading and transmission.

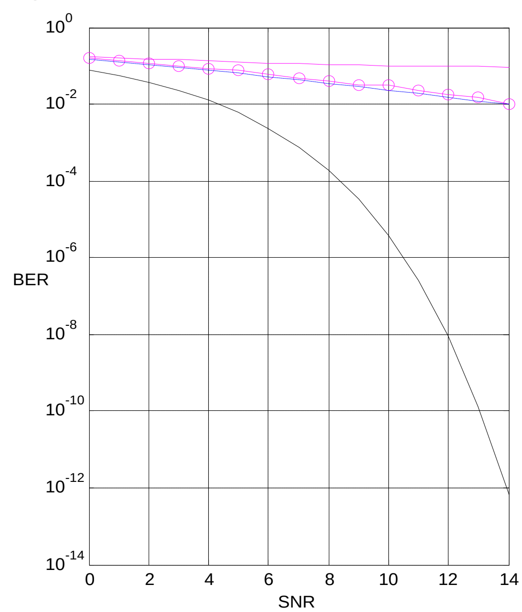

Fig. 5 BER curves for the receiver in presence of AWGN and fading: theoretical (magenta) and simulation (magenta cycles) for fading and theoretical for noise only (black).

As expected, the BER rate in fading channel is significantly greater than in the case when AWGN only is present in the channel (black curve). For the sake of comparison, the BER for Standard binary sequences [7] are compared by the BER for chaotic sequences of the same average powers. The BER in the case when a chaotic sequence is used is slightly worse than in the case when a binary orthogonal chip sequence defined by the Standard for wireless sensor networks is used. The BER in presence of fading is significantly worse than in the case when only AWGN is present in the channel (Black curve in Fig. 5). This degradation in BER due to fading can be eliminated by using one of the diversity methods. In order to eliminate this degradation of BER in fading, a method of fading mitigation using interleavers is investigated in the next section of this paper.

IV. INTERLEAVER COMMUNICATION SYSTEM

In real wireless systems the influence of fading on signal transmission can be very high that is manifested as severe attenuation of the signal received. Therefore, it is important to mitigate this fading influence. Various diversity schemes can be used for this mitigation [11]. It was shown that the interleaver and deinterleaver blocks at the transmitter and the receiver side, respectively, can also mitigate Rayleigh fading in direct sequences spread spectrum systems [4, 13-15]. Therefore, in the communication system defined for wireless sensor networks, it will be worth to see if this interleaver technique can be applied.

The following theoretical analysis of the system presented in Fig. 2, the interleaver (IL) and deinterleaver (DI) blocks will be included into the transceiver structure and theoretically analyzed. It will be assumed that a simple block interleaver of 2βx2β size is employed. According to this interlaeaver structure, the chips for each bit will be written into the block interleaver row wise. Thus the first raw will contain all the chips belonging to the first bit. When the interleaver block is full the chips will be taken out column wise and applied to the input of the modulator. Thus, the first 2β chips entering the modulator will belong to 2β different bits.

The opposite operation is performed by the deinterleaver at the receiver side to re-order the chips. Namely, the first 2β chips taken out of the deinterleaver will contain the chips belonging to the fist bit but affected by different fading coefficients. By this operation the samples of chips z_i at the output of multiplexer (MUX) are practically affected with independent fading coefficients and can be expressed as

$$z_i = \alpha_i \sqrt{E_c} \cdot c_{i1} + \sqrt{E_N} \cdot n_i \, . \tag{29}$$

These are soft chip values that are applied at the chip sequence correlator input, which consists of a multiplier and an adder. For the assumed first bit value equal to +1, which is sent at the transmitter side, the output of the correlator is a sum of 2β chip samples, which can be represented as one realization of a random variable W_1, expressed as

$$w_1 = \sum_{i=1}^{2\beta} z_i c_{i1} = \sqrt{E_c} \sum_{i=1}^{2\beta} \alpha_i c_{i1}^2 + \sqrt{E_N} \sum_{i=1}^{2\beta} n_i \cdot c_{i1} = A + B \tag{30}$$

This is a bit soft value. The mean and variance of this random variable are

$$\eta_{w_1} = E\{w_1\} = \sqrt{E_c} \sum_{i=1}^{2\beta} E\{\alpha_i\} E\{c_{i1}^2\} \tag{31}$$

and

$$\sigma_{w1}^2 = E_c [\sum_{i=1}^{2\beta} E\{\alpha_i^2\} E\{c_{i1}^4\} - \sum_{i=1}^{2\beta} E^2\{\alpha_i\} E\{c_{i1}^2\}] \, . \\ + 2\beta E_N E\{c_{i1}^2\} \tag{32}$$

If the expectations (7), (8) and expectation for Rayleigh variable are inserted into (31) and (32), the mean and the variance of a bit soft value can be simplified to

$$\eta_{w_1} = 2\beta \sqrt{\pi / 4} \sqrt{E_c} \tag{33}$$

and

$$\sigma_{w1}^2 = 2\beta E_c [\frac{6-\pi}{4} + \frac{N_0}{2E_c}] \, . \tag{34}$$

Due to the CL theorem, the random variable representing bit soft value has Gaussian distribution having the mean (33) and variance (34). Therefore, for the binary message bits and chaotic spreading sequences with unit average power, the probability of error can be expressed as

$$p_{be} = \frac{1}{2} erfc \left[\frac{(6-\pi)}{\beta\pi} + \frac{4}{\pi} \left(\frac{E_b}{N_0} \right)^{-1} \right]^{-1/2} . \tag{35}$$

Simulators were developed in MATLAB to investigate characteristic of communication systems that includes the interleaver/deinterleaver structure and the achieved improvements in BER due to the interleaver application is presented in Fig. 6 (dashed magenta). This BER curve is plotted according to the theoretical expression (35). For signal to noise ratio SNR = 8, for example, the theoretical gain in BER rate is from $2\text{x}10^{-2}$ to $1.8\text{x}10^{-3}$. This improvement in BER substantially increases when signal to noise ratio increases. The theoretical curve with interleaver and deinterleaver blocks, according to expression (35), is plotted in magenta, while the curve for AWGN presence in the channel is presented in black colour. For the BER value that is approximately $2\ \text{x}10^{-2}$, the saving in SNR is approximately 5.5 dB, as shown in Fig. 6. This saving increases significantly when the BER decreases.

It is interesting to compare the theoretically derived expressions for the BER with the corresponding graphs obtained by simulation. The theoretical expression (35) is confirmed by the simulation of the system as the results presented in Fig. 7 show. Obviously, the theoretical curve, based on the closed form derivative (35), is followed by the BER curve obtained by simulation. The difference between the two curves, being less than 0.2 dB, is negligible.

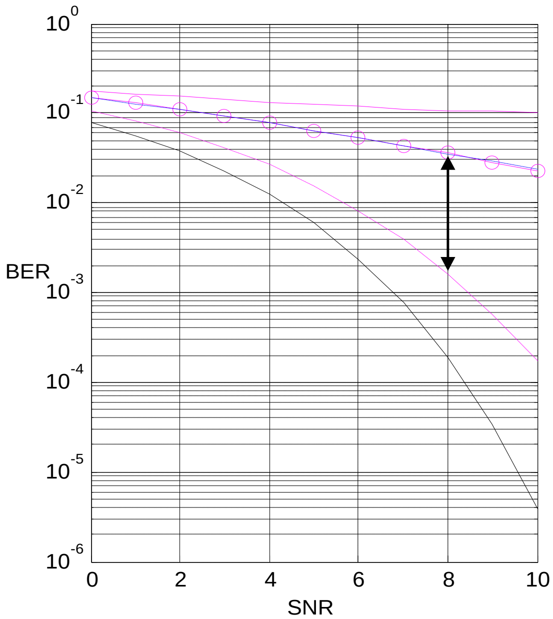

Fig. 6 BER curves for the system with inteleaver and deinterleaver in AWGN and fading channel: theoretical for fading (Blue), theoretical for fading with interleavers (Red) and theoretical for noise only (Black).

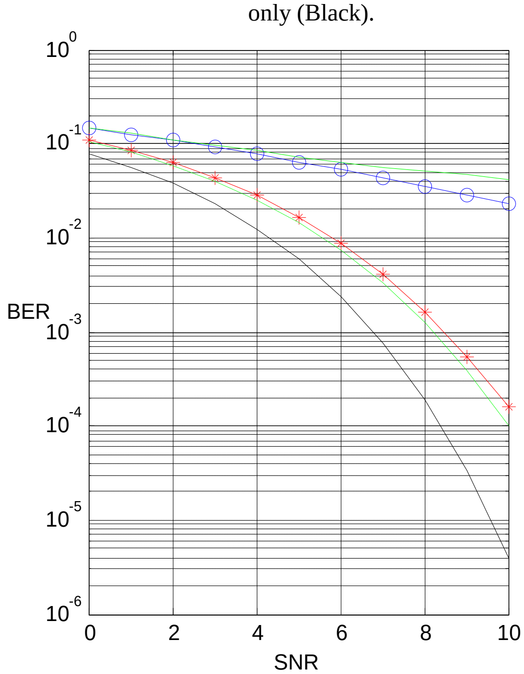

Fig. 7 BER curves inteleaver receiver in presence of AWGN and fading: theoretical (Blue) for fading, theoretical derived (Green full line) theoretical with interleavers (Green dashed) followed by the simulation (Red) for fading with interleavers and theoretical curve for noise only (Black).

We can conclude that, by using interleavers the fading coefficients are de-correlated and the fading influence becomes similar to the influence of the AWGN. Consequently, the fading BER curve comes closer to the curve that is obtained when only AWGN noise is present in the channel. Further improvements in BER could be achieved if the spreading factor 2β is increased, as can be seen from theoretical expression (35). Therefore, the general conclusion is that the block chip interleaving is an efficient technique that can be used to mitigate fading in the physical channel of wireless sensor networks [17]. Also, further investigation can target the other kind of interleavers and their efficiency in respect to the fading mitigation. To achieve desired accuracy of BER, in all previous graphs, estimation the number of chips and bits in the simulation are chosen according to the requirements presented in reference [16].

V. Conclusion

In this paper, the theoretical expressions for the probability of errors are derived for a communication system representing the physical layer of wireless sensor networks. The system is analyzed in the case when flat fading is present in the channel and in the case when the interleaver technique is used to mitigate the fading. It was found that the interleaver technique mitigates the fading and significantly improves the BER rate in the system. For example, for SNR = 8 dB, the theoretical gain in BER rate achieved is from 2×10^{-2} to 1.8×10^{-3}. The communication system analyzed has a structure that is defined for the wireless sensor network applications. In the theoretical analysis and in simulation, all the signals are represented and processed in discrete time domain. In this way the developed and simulated system model can be easily implemented in digital technology, DSP or FPGA.

References

[1] Lee, S. J. and Miller, L. E., CDMA Systems Engineering Handbook, 1st edition, Artech House Publishers, Boston and London, 1998.
[2] X. Gui, Chip-Interleaving DS SS System over Rician Multipath Fading Channel, Wireless Communication and Mobile Computing, John Wiley & Sons, on-line, DOI/wcm.1230, 2011.
[3] R. H. Mahadevappa and J. G. Proakis, Mitigating multiple access interference and intersymbol interference in uncoded CDMA systems with chip-level interleaving, IEEE Trans. on Wireless Communications, vol. 1, 2002, pp. 781-792.
[4] S. M. Berber, R. Vali, Fading Mitigation in Interleaved Chaos-Based DS-CDMA Systems for Secure Communications, 15th WSEAS Int. Conf. on Communications, Corfu, Greece, July 15-17, 2011, pp. 1-6.
[5] L. Yu-Nan and D. W. Lin, Novel analytical results on performance of bit-interleaved and chip-interleaved DS-CDMA with convolutional coding, IEEE Transactions on Vehicular Technology, Vol. 54, 2005, pp. 996-1012.
[6] X. Gui and T. S. Ng, A Novel chip-Interleaving DS SS System, IEEE Trans. On Veh. Tech., Vol. 49, January 2000, pp. 21-27.
[7] "IEEE Std 802.15.4-2006 (Revision of IEEE Std 802.15.4-2003), Wireless Medium Access Control (MAC) and Physical Layer (PHY) Specifications for Low-Rate Wireless Personal Area Networks (WPANs), pp. 0_1-305, 2006.
[8] C. C. Wang, C. C. Huang, J. M. Huang, C. Y. Chang, C. P. Li, Zig-Bee 868/915-MHz Modulator/Demodulator for Wireless Personal Area Network, IEEE Transactions on Very-Large Scale Integration (VLSI) Systems, Vol. 16, No. 7, July 2008, 936-938.

[9] O. Nam-Jin, L. Sang-Gug, Building a 2.4-GHZ radio transceiver using IEEE 802.15.4, Circuits and Devices Magazine, IEEE, Vol. 21, 2006, pp. 43-51.

[10] G. Kaddoum, D. Roviras, P. Charge, and D. Fournier-Prunaret, Robust synchronization for asynchronous multi-user chaos-based DS-CDMA, Signal Processing, vol. 89, no. 5, pp. 807–818, 2009.

[11] M. Bank, Y. Barish, S. Tapuchi, M. Bank, B. Hill, M. Haridim, Phase Diversity Method in Mobile Communication Systems, International Journal of Communications, Issue 2, vol. 6, pp. 64–71, 2012.

[12] R. Vali, S. Berber, and S. K. Nguang, Effect of Rayleigh fading on non-coherent sequence synchronization for multi-user chaos based DS-CDMA, Signal Processing, vol. 90, no. 6, pp. 1924–1939, 2010.

[13] H. Torii, M. Satoh, T. Matsumoto, and M. Nakamura, Quasi-Optimal and Optimal Generalized Mutually Orthogonal ZCZ Sequence Sets Based on an Interleaving Technique, International Journal of Communications, Issue 1, vol. 7, pp. 18–25, 2013.

[14] Stevan M. Berber, Ramin Vali, *Fading Mitigation in Interleaved Chaos-Based DS-CDMA Systems for Secure Communications*, 15th WSEAS Int. Conf. on Communications, Corfu, Greece, July 15-17, 2011, pp. 1-6.

[15] B. K. Upadhyaya, and S. K. Sanyal, Novel design of WiMAX multimode interleaver for efficient FPGA implementation using finite state machine based address generator, International Journal of Communications, Issue 2, vol. 6, pp. 27–36, 2012.

[16] S. M. Berber, Bit error rate measurement with predetermined confidence, Electronics Letters, vol. 27, p. 1205, 20th June 1991.

[17] S. Berber, S. Feng, Chaos-Based Physical Layer Design for WSN Applications, 17th WSEAS Int. Conf. on Communications, Rhodos, Greece, July 16-19, 2013, pp. 1-6.